General Disclaimer

One or more of the Following Statements may affect this Document

- This document has been reproduced from the best copy furnished by the organizational source. It is being released in the interest of making available as much information as possible.

- This document may contain data, which exceeds the sheet parameters. It was furnished in this condition by the organizational source and is the best copy available.

- This document may contain tone-on-tone or color graphs, charts and/or pictures, which have been reproduced in black and white.

- This document is paginated as submitted by the original source.

- Portions of this document are not fully legible due to the historical nature of some of the material. However, it is the best reproduction available from the original submission.

Produced by the NASA Center for Aerospace Information (CASI)

DRA

(NASA-CR-173354) CENTRIFUGE IMPACT CRATERING EXPERIMENT 5 Semiannual Report (Boeing Aerospace Co., Seattle, Wash.) 39 p HC A03/MF A01 CSCL 14B

N84-19784

Unclas

G3/35 00610

SEMI-ANNUAL REPORT

15 JANUARY 1984

ATTN: EL-4

CENTRIFUGE IMPACT CRATERING EXPERIMENT V:

NASW-3291

MAR 1984
RECEIVED
NASA STI FACILITY
ACCESS DEPT.

This work is sponsored by:

NASA Planetary Geophysics
Office of Space Science
Washington, D.C. 20546

Boeing Aerospace Company
Seattle, Washington 98124

FASTAX II CAMERA FRAMING RATES VS GRAVITY

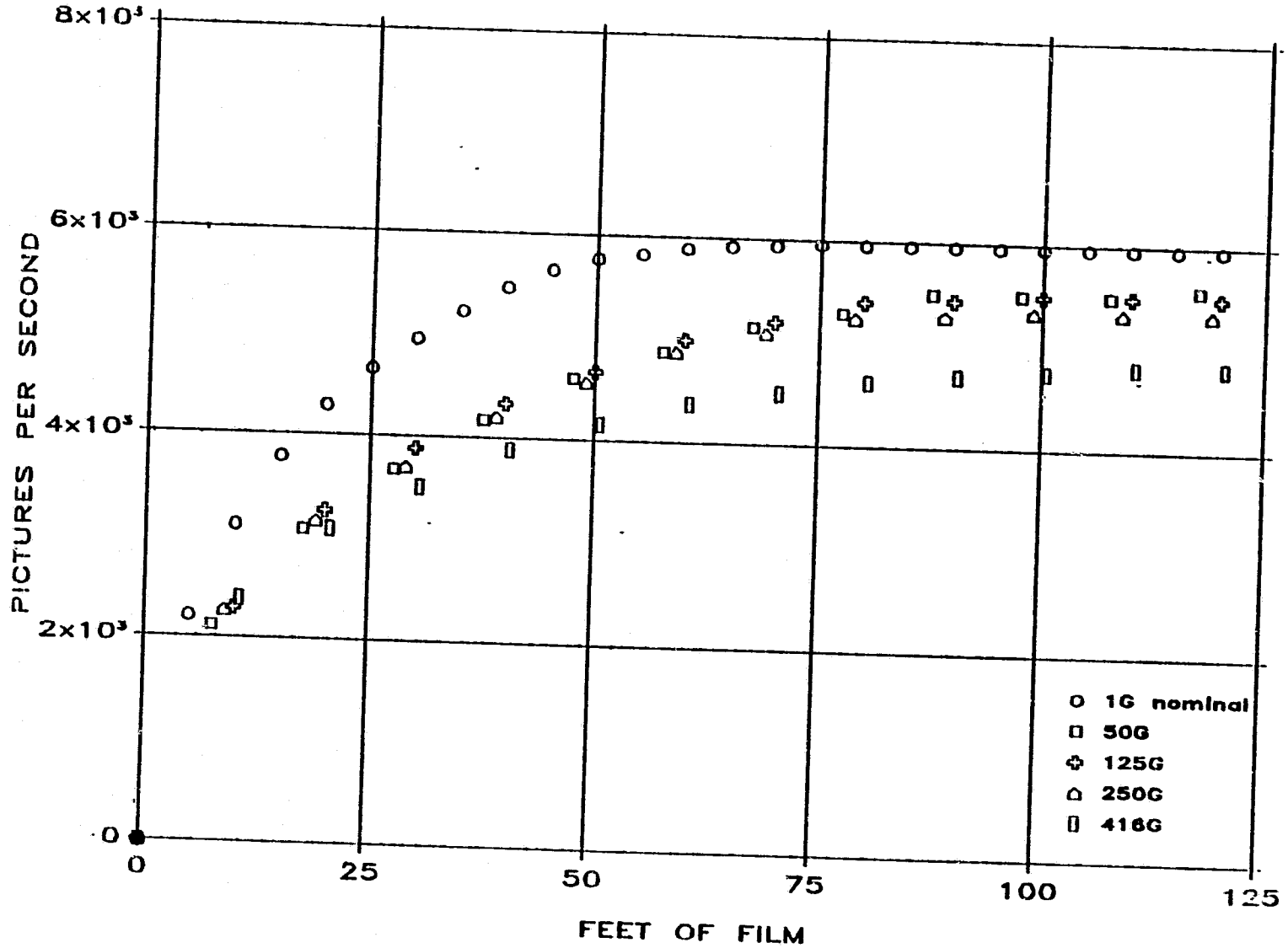

ORIGINAL PAGE IS
OF POOR QUALITY

TRANSIENT CRATER MOTIONS: SATURATED SAND CENTRIFUGE EXPERIMENTS

Schmidt, R. M., Boeing Aerospace Company, M/S 13-20, Seattle, WA 98124

The kinematics of crater formation are being investigated using a quarter-space test bed on a centrifuge. This technique (1) allows high-speed movie coverage of target deformations as seen in cross section through a 2-inch Plexiglas window along a diametrical symmetry boundary. The data for the eight shots performed to date with the recently installed Fastax II-100 rotating-prism camera are shown in the attached table. Two objectives of these tests were to dynamically record the maximum depth of the transient crater and to record its collapse. Preliminary interpretation of the film records for shot 307-QXE is shown in the attached figure. This shot was conducted in nearly-saturated moderately-dense fine-grained Ottawa "Banding" sand.

For this target material, crater floor uplift ("collapse") occurs on the same time scale as the radial motion of the ejecta plume. Because of the impairment of the optical path due to detonation products plating onto the window, the floor uplifting sequence could not be resolved in some of the intermediate frames of the work print. It appears to be complete by frame 21 and maybe earlier. At this time the ejecta plume is in the vicinity of the final apparent crater radius and the crater profile is in agreement with the final apparent crater measured after the shot with the profilometer. Crater volume displays power-law growth until maximum transient depth occurs (frame 4). More interestingly crater radius shows power-law growth all the way out to final crater radius (frame 21). Both time exponents, interpreted with the assumption of a unique coupling parameter, $6\alpha/(3+\alpha)$ for volume and $2\alpha/(3+\alpha)$ for radius, are in good agreement with a value of the gravity exponent α equal to 0.65. This same value was determined for crater growth in water (2) (3) and may be applicable for all non-porous geological targets.

As an expedient when determining the maximum charg[illegible] that would not spall or puncture the window, the explosive charges were built up [illegible] Dupont Deta-Sheet. This is PETN with approximately 25% inert plastic filler, which is presumed to cause much of the smoke and detonation debris products. Pure PETN is now under consideration for future shots to improve resolution by reduction of smoke and opaque detonation products. However, since the Deta-Sheet detonation products deposit on the window as it is exposed to the transient crater, a permanent record of the envelope of maximum crater depth versus range is formed. Preliminary comparisons of the detonation product profile with the corresponding final apparent crater profile along with viewing the films indicate that there was no significant difference in the transient crater phenomena over a variation of approximately an order of magnitude in sand grain size. This observation needs further examination when the original film records are digitized.

For seven of the eight shots, the water table was nominally at 1.05 cm below the original ground zero. This was to correspond to the approximate scale of the 500-ton PRAIRIE FLAT explosive crater in the field, which was modeled in the tangent-above shot 306-QXE (see ref. 4).

(1) Schmidt, R. M. & Piekutowski, A. J. (1983) Lunar & Planetary Science XIV, p. 668.
(2) Schmidt, R. M. & Holsapple, K. A. (1982) Estimates of crater size for large-body impact: Gravity-scaling results. Geol. Soc. of America SP 190, p. 93.
(3) Schmidt, R. M. (1983) Trans. Am. Geophys. U. (EOS) Vol. 64, No. 45, p. 747.
(4) Schmidt, R. M., Fragaszy, R. J. & Holsapple, K. A. (1981) Proc. of Seventh Int. Symp. on Military Applications of Blast Simulation, Medicine Hat, Canada, p. 4.2-1.

TRANSIENT CRATER MOTIONS: SATURATED SAND CENTRIFUGE EXPERIMENTS

Schmidt R. M.

QUARTER-SPACE DATA TABLE

		EXPLOSIVE			MATERIAL		CRATER				π-GROUPS				
Shot No. –	Gravity (G)	Mass (gm)	Q (Cerg/g)	Density (g/cc)	Type –	Density (g/cc)	V (cm^3)	r (cm)	h (cm)	h_T* (cm)	π_2 –	π_v –	π_r –	π_h –	π_{hT}* –
306-QXE**	399	13.0	38.5[4]	1.48	WBS[1]	2.06	232	8.64	2.08	–	2.10×10^{-5}	36.8	4.67	1.13	–
307-QXE	400	4.45	38.5	1.48	WBS	2.06	289	8.86	2.77	4.68	1.47×10^{-5}	134	6.85	2.14	3.62
319-QXE***	403	5.49	42.5[5]	1.45	WBS	2.06	232	7.45	2.95	–	1.45×10^{-5}	87.1	5.37	2.13	–
324-QXE	398	4.23	42.5	1.45	WBS	2.06	202	7.21	2.60	–	1.31×10^{-5}	98.4	5.67	2.05	–
326-QXE	398	4.14	42.5	1.45	WBS	2.06	212	7.75	2.40	–	1.30×10^{-5}	105	6.14	1.90	–
328-QXE	401	4.25	42.5	1.45	WFS[2]	2.11	193	7.41	2.17	3.64	1.32×10^{-5}	95.8	5.87	1.72	2.88
329-QXE	100	4.14	42.5	1.45	WBS	2.06	392	9.76	3.25	6.55	3.27×10^{-6}	195	7.73	2.58	5.19
330-QXE	100	4.19	42.5	1.45	WFF[3]	1.97	320	8.04	3.49	5.90	3.29×10^{-6}	150	6.25	2.71	4.59

* Maximum Transient Crater Depth ** Tangent Above – all others Tangent Below *** Water Table = 0.70cm
[1] WBS = Wet Banding Sand (212μ) [2] WFS = Wet Flintshot Sand (800μ) [3] WFF = Wet F-140 Sand (106μ)
[4] Green Data-Sheet (Type C) [5] Red Data-Sheet (Type D)

SHOT 307-QXE TRANSIENT CRATER FORMATION 400G

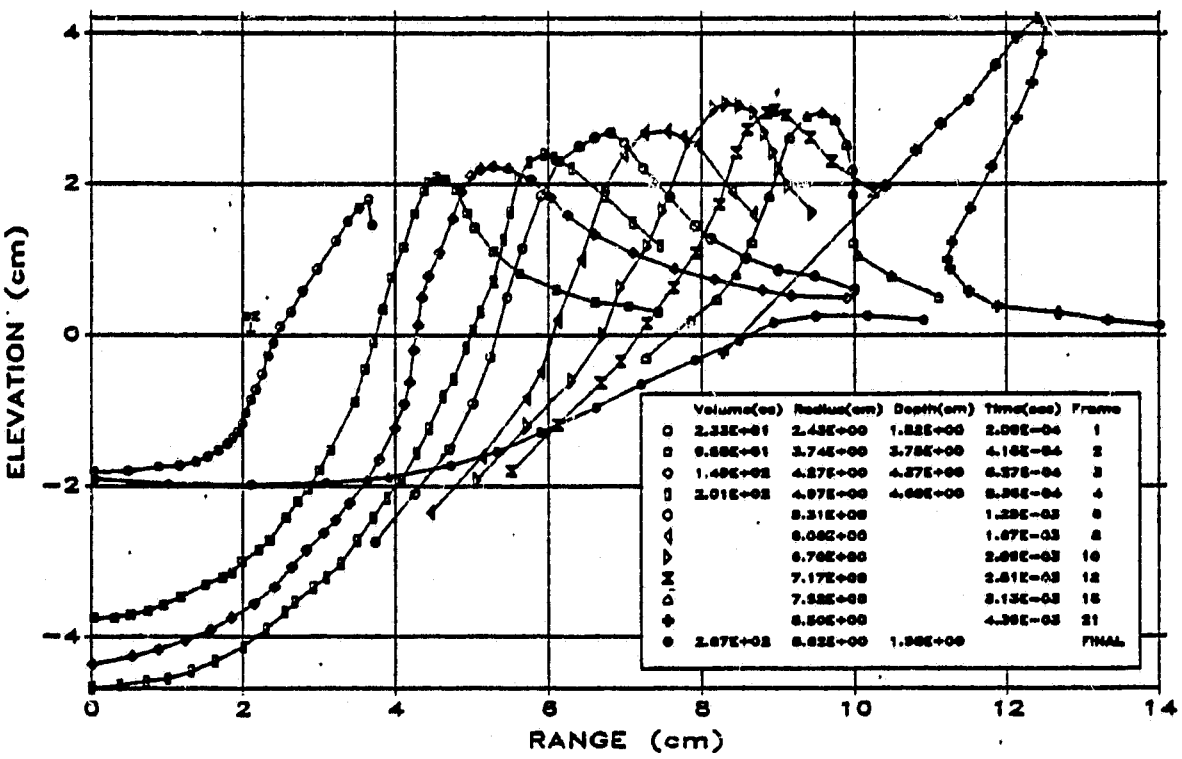

ORIGINAL PAGE IS
OF POOR QUALITY

Cratering Flow Fields: A General Form and the Z Model

Kevin Housen, Shock Physics and Applied Mechanics, MS 13-20, Boeing Aerospace, Seattle, WA, 98124.

The nature of material motions is often fundamental in discussions of impact-related processes. An analytic description of cratering flow fields, known as the Z model, was developed by Maxwell and Seifert (1974). Although originally developed for near-surface explosions, it has also been used in calculations of impact ejecta velocities, transient craters and melt generation (e.g., Schultz and Gault, 1979; Croft, 1980; Grieve and Cintala, 1981). While it reasonably describes the flow field in some cases (e.g. Orphal *et al*, 1977), in others it does not. A more general expression for flow velocity is developed here which, in certain instances, reduces to a Z model.

Z Model

The Z model was based on a series of numerical simulations of cratering events. Briefly, the radial velocity of material behind the outgoing shock wave was observed to vary as a power of the radial position r. Discussions of the Z model often include a time dependent term so that

$$\dot{r} = A(t)\, r^{-Z} \qquad (1)$$

where A(t) describes the time dependence of the flow. After the passage of the shock, the material density was found to be nearly constant. The observed incompressibility can be used with eq (1) to determine the tangential velocity component (e.g. Maxwell, 1977):

$$r\dot{\vartheta} = \dot{r}\,(Z-2)\,\sin(\vartheta)/\{1+\cos(\vartheta)\} \qquad (2)$$

where ϑ is the angle measured from the downward axis ($\vartheta=0$ vertically down and $\vartheta=\pi/2$ along the target surface). Note that material flows upward toward the surface when $Z>2$ ($\vartheta>0$) and downward away from the surface when $Z<2$ ($\vartheta<0$). Radial flow occurs when $Z=2$.

Once A(t) is specified, eqs (1) and (2) determine, among other things, the temporal growth of the crater (Maxwell, 1977). A case often adopted in the literature is that of steady flow, where A is independent of time. In this case, the radius, $R_c(t)$ of the expanding crater is

$$R_c(t) \propto t^{1/(Z+1)} \qquad (3)$$

Measurements of crater growth in a variety of materials show that, indeed, crater radius grows as a power of time (e.g. Schmidt, 1983,1984; Holsapple, 1984). However, for some materials, steady flow cannot hold. For example impacts and explosions in water and wet sand targets (Schmidt, 1984) imply R_c grows as $t^{0.36}$, corresponding to $Z=1.8$. But, as noted above, the flow field is rotational away from the surface for $Z<2$. Consequently, a steady flow Z model cannot apply to these cases.

Austin *et al* (1980) have compared numerical simulations of impact in plasticene clay to predictions based on the Z model. They found it necessary to modify the basic form of the Z model. The flow center had to be located beneath the surface and both A and Z increased with time. In particular, Z was somewhat less than 2 early on and steadily increased to values between 3 and 4, depending on ϑ. Austin *et al* concluded that the Z model "should only be applied with caution to impact cratering". A more general description of cratering flow fields is considered next.

Implications of a Coupling Parameter

The cratering process can be conceptually divided into three phases: (1) an early-time phase, where the impactor energy and momentum are coupled into the target; (2) an intermediate phase where coupling has taken place but the effects of gravity and target strength are small; (3) a late-time phase where gravity and strength begin to slow the crater growth. Searches have been made for a measure of "late stage equivalence" whereby a single measure of the early-time coupling phase could be used to predict the intermediate and late-stage behavior. Holsapple (1981, 1984) has generalized and quantified this idea by introducing a "coupling parameter" which, subsequent to the early-time phase, conveys all information about the impactor. This concept has been used to construct scaling laws for crater ejecta (Housen *et al*, 1983) and will now be used to investigate the nature of cratering flow fields.

Suppose that, in the intermediate time regime, the radial velocity of material depends on the impactor radius, velocity and density (a, U and δ) and the target density, ρ, in addition to the position coordinates (r,ϑ) and the time t. The late time regime, where gravity or material strength are important, is not considered here. Using a coupling parameter, the radial velocity can be written as

ORIGINAL PAGE IS
OF POOR QUALITY

ORIGINAL PAGE IS
OF POOR QUALITY

$$\dot{r} = F(\, C,\ \rho,\ r,\ \vartheta;\ t) \qquad (4)$$

where F is an unspecified function and the coupling parameter, C, is a scalar-valued function of a, U and δ. A dimensional analysis of (4) gives

$$\dot{r}/U = (r/a)^{-\beta}\ \mathcal{F}\{\ \vartheta,\ (r/a)^{-\beta-1}\ Ut/a\ \} \qquad (5)$$

where $\mathcal{F}$ is an unspecified function and, for convenience, the density ratio ρ/δ is assumed constant. The exponent β is related to the dimensions of the coupling parameter and can be predicted from the measured dependence of final crater size on initial conditions. In particular, β should be about 2.5 for porous targets (e.g. dry sand) and 1.8 for nonporous targets (e.g. water, saturated sand, metals).

In general, the time dependent Z model as given in eq (1) is not consistent with a coupling parameter because eq (1) implies a product of separate functions of r and t whereas eq (5) does not. However, there is a special form of the Z model which is admitted by a coupling parameter: the function A(t) in eq (1) varies as a power of time. Consider the three following cases, listed in order of decreasing generality.

1. If A(t) is assumed to vary as a power of t, say t^{γ}, then the Z model can be viewed as a "local approximation" to a coupling parameter. That is, for a small interval of time, the function in eq (5) can be approximated locally (in log-log space) by $\mathcal{F} \propto \{(r/a)^{-\beta-1}\ Ut/a\}^{\gamma}$, where γ may vary with time. Locally, the exponents are related by $Z=\beta+\gamma(\beta+1)$. Note, if γ varies with time then so will Z (β is constant for a fixed material).

2. If $\mathcal{F}$ has the special form of a power law, i.e., if γ is independent of time, then eq (5) reduces to a Z model (again, where A is proportional to t^{γ}).

3. In the special case of steady flow, the Z model corresponds to a coupling parameter with $Z=\beta$.

Case 1 may explain, at least qualitatively, the observations of Austin *et al* (1980) that both A and Z (in eq 1) increased with time. If, for the case studied by Austin *et al*, $\mathcal{F}$ was not a power law and the *local* slope of $\mathcal{F}$ (i.e., γ) started out near zero and increased with time, then Z would start out near 1.8 and would increase with time (note, $\beta \simeq 1.8$ is expected for their clay target). A coupling parameter may explain the observations of Austin *et al*. But without specific knowledge of the time dependence observed in their computed flow field it is difficult to perform a rigorous test.

Piekutowski's (1980) measurements of particle velocities for a small-scale explosion in dry sand are shown below in the form consistent with eq (5). While there is some scatter due to measurement error, the data for various "tracer particles" follow a common trend. Hence, a coupling parameter scales these data rather well. Piekutowski's results imply that $\mathcal{F}$ is a decreasing function of time for dry sand, while $\mathcal{F}$ increased with time in the Austin *et al* calculations. This raises the possibility that $\mathcal{F}$ may differ markedly for different materials.

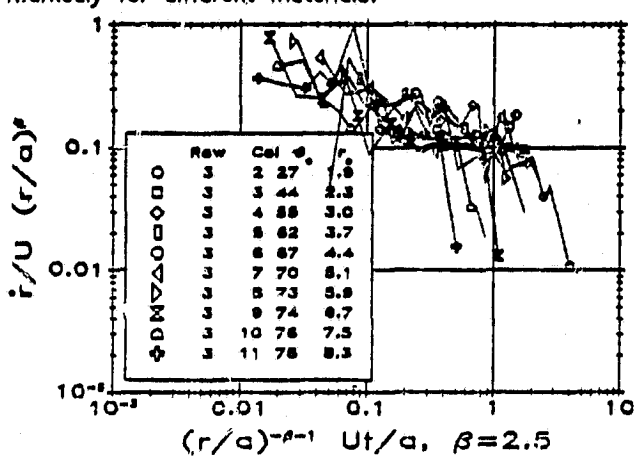

Scaled particle-velocity measurements for dry sand (Piekutowski, 1980).

REFERENCES: Austin,M.G., Thomsen,J.M., Ruhl,S.F., Orphal,D.L., and Schultz,P.H.(1980), Proc LPSC 11th, 2325–2345. Croft,S.K. (1980), Proc LPSC 11th, 2347–2378. Grieve,R.A.F. and Cintala,M.J. (1981), Proc LPSC 12th, 1607–1621. Holsapple,K.A. (1981), EOS, 62, 949. Holsapple,K.A. (1984) Abstract, this volume. Housen,K.R., Schmidt,R.M. and Holsapple,K.A. (1983), JGR, 88, 2485–2499. Maxwell,D. and Seifert,K.(1974), Report DNA 3628F. Maxwell,D.(1977) in Impact and Explosion Cratering, 1009–1024. Orphal D.L.(1977)in Impact and Explosion Cratering, 907–917. Piekutowski A.J.(1980) Proc LPSC 11th, 2129–2144. Schmidt,R.M.(1983) EOS, 64, 747. Schmidt,R.M.(1984) Abstract, this volume. Schultz,P.H. and Gault,D.E. (1979), JGR, 84, 7669–7687.

ORIGINAL PAGE IS
OF POOR QUALITY

ON CRATER DYNAMICS: COMPARISONS OF RESULTS FOR DIFFERENT TARGET AND IMPACTOR CONDITIONS

K. A. Holsapple, University of Washington FS-10
Seattle, WA 98195

A fundamental question of impact cratering mechanics is how the impactor and target conditions and material properties affect the crater. This question must be answered in order that known results can be extrapolated with confidence to new and different cases.

Recent studies have uncovered a surprising simplicity in a large number of cratering problems. This simplicity is a consequence of a separation of the early from the intermediate and late-time mechanics, with a single scalar-valued "coupling parameter" depending on impactor radius a, velocity U and mass density δ, as $C \propto a U^{\mu} \delta^{\nu}$, being the sole measure of the impactor for all of the intermediate to late-time processes. Previous applications to final crater geometry (1,2), to ejecta blankets (3) and to crater formation time (4) have been reported.

Here the entire dynamical history of crater growth is considered. Fig. 1 shows the crater depth d versus time t for a wide variety of experimental and calculated craters in non-porous targets (5-10), as well as new results for impacts into aluminum. The targets include metals, rock, clay and water and the impactors range over a variety of materials with the mass densities from 0.01 to 8 gm/cm^3. The impact velocities range from 2.5 to 100 km/sec. The results span many decades in size and time.

Each of these growth curves shows at least some aspects of a generic crater depth versus time curve as sketched in Fig. 2, showing three identifiable regimes. In the very early time, the flow is one-dimensional and there is no dependence on impactor radius. The crater growth proceeds simply as $d = vt$ where v is the initial target particle velocity determined by U and the impedances of the two materials.

As the flow becomes two-dimensional, the impactor radius becomes an important parameter. However, after a very short transition time, the sole remaining measure of the impactor is the value of the coupling parameter C given above. The exponents μ and ν are found to be $\mu = 0.58$ and $\nu = 0.66$ for all of the cases shown, and the crater growth can be shown to be governed by the law $d \propto t^{\mu/(1+\mu)}$.

Finally, in the late-stages, the growth is inhibited by either material strength Y (in the case of small craters) or by gravity g (in the case of large craters; $\rho g d >> Y$) and the scaling of the maximum crater size is governed by the results reported previously.

These results imply that, in each regime, a different scaling exists that should relate all crater histories. Figures 3, 4, and 5 illustrate this fact showing respectively, the early, intermediate and late-time scaling. In each case, the variety of curves do indeed superimpose in the applicable regime.

ORIGINAL PAGE IS
OF POOR QUALITY

ON CRATER DYNAMICS

K. A. Holsapple

1. Holsapple,K.A.(1981) Coupling parameters in cratering (abstract). In EOS 62, p.949.
2. Holsapple,K.A.(1983) On the existance and implications of coupling parameters in cratering mechanics (abstract). In Lunar and Planetary Science XIV,pp.319-320.
3. Housen,K.R.,Schmidt,R.M.,Holsapple,K.A.(1982)J. Geophys. Res. 88(B3), pp.2485-2499.
4. Schmidt,R.M.(1981) Scaling crater time of formation (abstract). In EOS 62,No45,p944.
5. Dienes,J.K.,Walsh,J.M.(1970) In High Velocity Impact Phenomena., ed. by R.Kinslow, Academic Press, New York, pp45-104.
6. Gault,D.E.,Sonnet,C.P.(1981) In Geological Implications of Impacts of Large Asteroids and Comets on the Earth. ed.by L.T.Silver and P.H.Schultz.
7. Kineke,J.H.,(1961) Observations of crater formation in ductile materialr. In Proceedings of the 5th Symposium On Hypervelocity Impact,vol.1, part 2, pp339-370.
8. O'Keefe,J.D.,Ahrens,T.J.(1982) Cometary and Meteorite Swarm Impacts on Planetary Surfaces. J. Geophys. Res.
9. Orphal,D.L., Borden,W.F., Larson,S.A., Shultz,P.H.(1980) Impact Melt Generation and Transport. In Proc. 11th Lunar and Planetary Science Conf., pp.2309-2323.
10. Austin,M.G., Thomsen,J.M., Ruhl,S.F., Orphal,D.L., Shultz,P.H.(1980) Calculational investigation of impact cratering dynamics: material motions during the crater growth period. In Proc.11th Lunar and Planetary Science Conf.,pp.2325-2345.

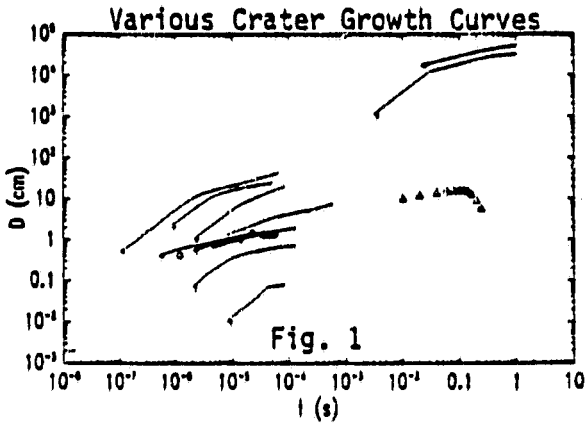

Fig. 1

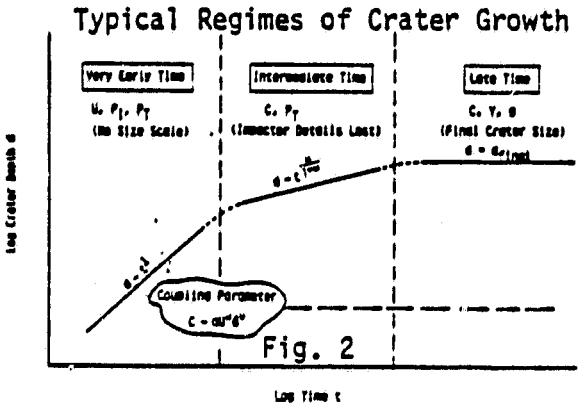

Fig. 2

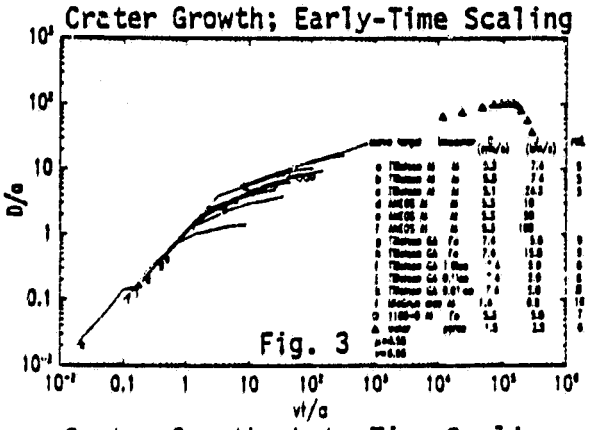

Fig. 3

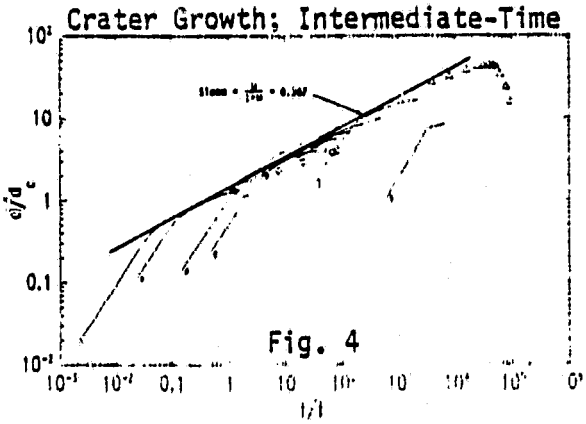

Fig. 4

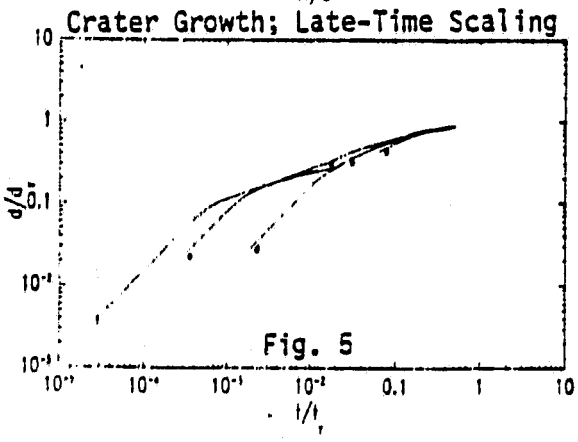

Fig. 5

ORIGINAL PAGE IS
OF POOR QUALITY

FEASIBILITY OF DETERMINING IMPACT CONDITIONS FROM TOTAL CRATER MELT

Michael D. Bjorkman, The Boeing Company, Seattle, WA 98124

In the past, authors have used parameters such as kinetic energy or momentum to scale crater volume and total melt volume (sum of that in crater and ejecta) produced by impact. The converse procedure; determining impact characteristics from, for example, the crater volume, will not determine impactor radius, a, and velocity, U, individually, but only as a product of powers of a and U. Recently, Grieve and Cintala (1) proposed to solve crater volume and total melt volume relations simultaneously to determine a and U individually for a terrestial crater. Their analysis pointed out that published total melt volume scaling relations varied from energy scaling (2) to momentum scaling (3), with no indication of the domain of applicability. The coupling parameter notion, described below, has the potential to unify the melt scaling relations and identify which materials nearly energy scale and which momentum scale.

The author examined the scaling of depth of melted planetary material along the axis of impact and showed (4) that a coupling parameter of the form $C = a\,U^{\mu}\,\delta^{\nu}$, $\mu = 0.58$, $\nu = 0.66$, which governs crater depth in nonporous materials like rocks and metals, also governs melt depth. The parameter δ is impactor density. This result necessarily follows from the fact that C determines sources which produce equivalent flow fields at intermediate and late times (5).

If the source variables a, U and δ only enter the scaling of melt depth D_m via C, then, $D_m = f(C, \rho, E_m)$, where ρ is the planet density and E_m is the specific energy of the Hugoniot state from which isentropic release ends at the 1 atm point on the liquidus. Dimensional analysis results in $D_m/a \propto (U^2/E_m)^{\mu/2}\ (\delta/\rho)^{\nu}$. Figure 1 is a plot of melt depths calculated with hydrocodes (2,6,7). If the above scaling relation holds, then the curve should be horizontal. Figure 1 shows that C does govern the melt depth for $v^2/E_m \geq 8$ (where v is the particle velocity at impact).

A similar analysis was performed for total melt volume (2,6-8) but did not demonstrate the coupling parameter governs melt volume. Figure 2 shows the data are not horizontal, and appear to be closer to energy scaling, $\mu = 0.67$. Perhaps crater and melt volume scale differently, however, this is difficult to understand, because they both stem from the same flow field, which has been shown to scale with $\mu = 0.58$ (9). The different scaling for the melt depth and melt volume is being looked into, and is suspected to result from free-surface effects.

The melt depth and melt volume scaling relations are both significantly different from momentum scaling, $\mu = 0.33$, however. The momentum scaling result (3) for total melt volume was obtained from an analytic model which prohibited ejection of material from the crater. This prevents multiplication of the downwards directed momentum and thus precludes any result other than momentum scaling. Momentum scaling of crater volume has been observed only for porous materials; it is therefore possible that the scaling relation from ref (3) applies to porous materials only.

If the present approach is correct, then it is not possible to distinguish the effects of the impactor radius and its velocity U separately using late time phenomena like total crater melt, crater dimensions or phase transitions in rocks below the crater. Only material from near the impact would retain information about a and U separately. Search for this material is complicated by ejection to great distances. Even if crater melt volume does scale with energy, $\mu = 0.67$ and crater volume with $\mu = 0.58$, the difference is not great enough to allow one to determine a and U separately to any useful accuracy.

FEASIBILITY OF DETERMINING IMPACT CONDITIONS FROM TOTAL CRATER MELT

Michael D. Bjorkman

1. Grieve, R. A. F. and Cintala, M. J. (1981) Proc Lunar Planet Sci 12th, p. 1607-1621.
2. O'Keefe, J. D. and Ahrens, T. J. (1977) Proc Lunar Sci Conf 8th, p. 3357-3374.
3. Gault, D. E. and Heitowit, E. D. (1963) in Proc 6th Hypervelocity Impact Symp. 2 p. 419-456.
4. Bjorkman, M. D. (1983) EOS (abstract), 64 (45) p. 747.
5. Bjorkman, M. D. and Holsapple, K. A. (1983). Proceedings of 3rd APS Conference on Shock Waves in Condense Media.
6. Holsapple, K A. (1984) On crater dynamics: Comparisons of results for different target and impactor conditions. This volume.
7. Orphal, D. L. et al (1980) Proc Lunar Planet Sci 11th, p. 2309-2323.
8. Bjork, R. L. et al. (1967), Analytical Study of Impact Effects as Applied to Meteoroid Hazard, NASA report CR-757.
9. Dienes, J. K. and Walsh, J. M., in High Velocity Impact Phenomena ed. by R. Kinslow (Academic Press, New York, 1970) p. 46-104.

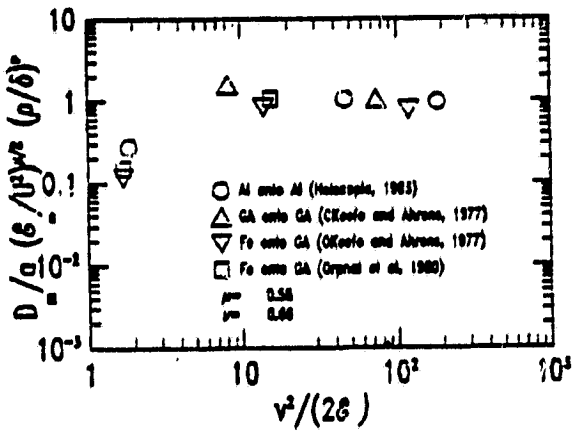

ORIGINAL PAGE IS
OF POOR QUALITY

Figure 1. Scaled melt depths.

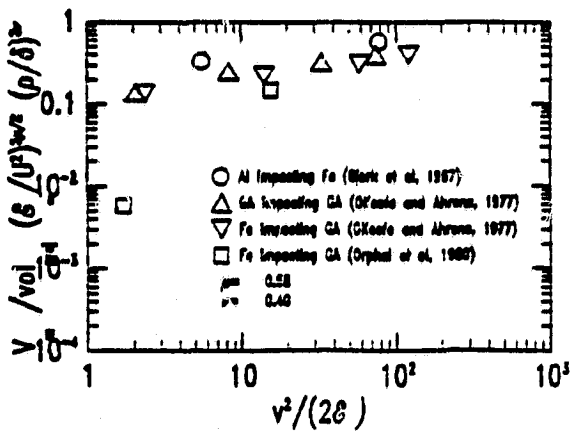

Figure 2. Scaled melt volumes.

CENTRIFUGE QUARTER–SPACE CRATERING RESULTS: A GRAVITY CRITERION FOR KINEMATIC SIMILARITY*

R. M. SCHMIDT, SHOCK PHYSICS LAB, M/S 13-20
BOEING AEROSPACE COMPANY, SEATTLE, WA 98124

THE SCALING OF IMPACT CRATER GROWTH*

K. A. HOLSAPPLE AND M. D. BJORKMAN
BOEING AEROSPACE COMPANY, SEATTLE, WA 98124

ORIGINAL PAGE IS
OF POOR QUALITY

* THIS WORK SUPPORTED BY NATIONAL AERONAUTICS AND SPACE ADMINISTRATION

PQ2-12

Centrifuge Quarter-Space Cratering Results
A Gravity Criterion for Kinematic Similarity

R. M. SCHMIDT
(The Boeing Co., M/S 13-20, Seattle, WA 98124)

Centrifuge cratering tests in water were performed using a quarter-space test bed. Transient cavity formation was recorded on 16-mm film at a framing rate of 5,000/sec. Each shot employed an E-106 detonating cap placed tangent-above on the water surface. These shots provided crater-growth histories for various gravities over the range of 10 to 916G. These histories are shown to be kinematically similar, when plotted in a non-dimensional form dictated by the assumption of gravity-scaled coupling parameter. Here V_G and T_G are the predicted values of maximum volume and time of formation. They depend only upon the exponent α obtained from the observed power-law dependence of the crater volume on the gravity-scaled size, V_g. For the explosion craters, α was assumed to be 0.63, which is the value obtained for projectile impact into water using the data of Gault and Sonett (GSA, SP130, 1973). Furthermore, with the same scaling, the impact data can be seen to superimpose with the explosion data.

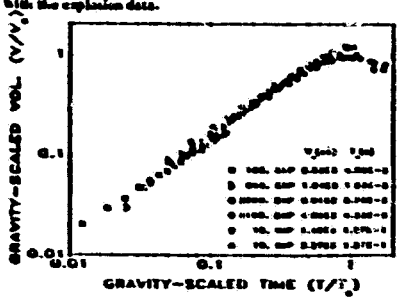

ORIGINAL PAGE IS
OF POOR QUALITY

Centrifuge Quarter-space Cratering Results: A Gravity Criterion for Kinematic Similiarity. (Results for Transient Cavity in Water)

Robert M. Schmidt
Boeing Aerospace Co.
Seattle WA 98124

8 December 1983

ORIGINAL PAGE IS
OF POOR QUALITY

1

ORIGINAL PAGE IS
OF POOR QUALITY

Centrifuge Quarter-Space Container

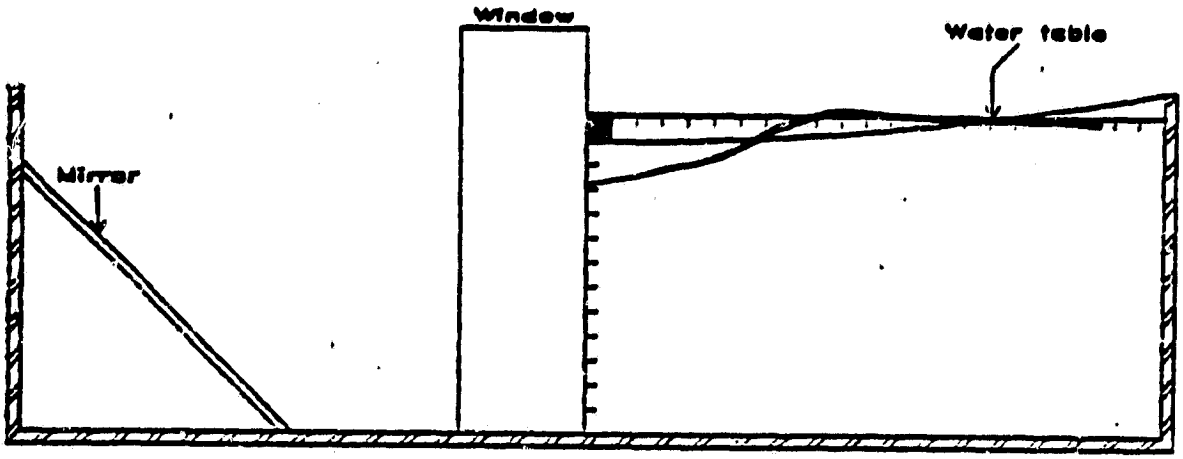

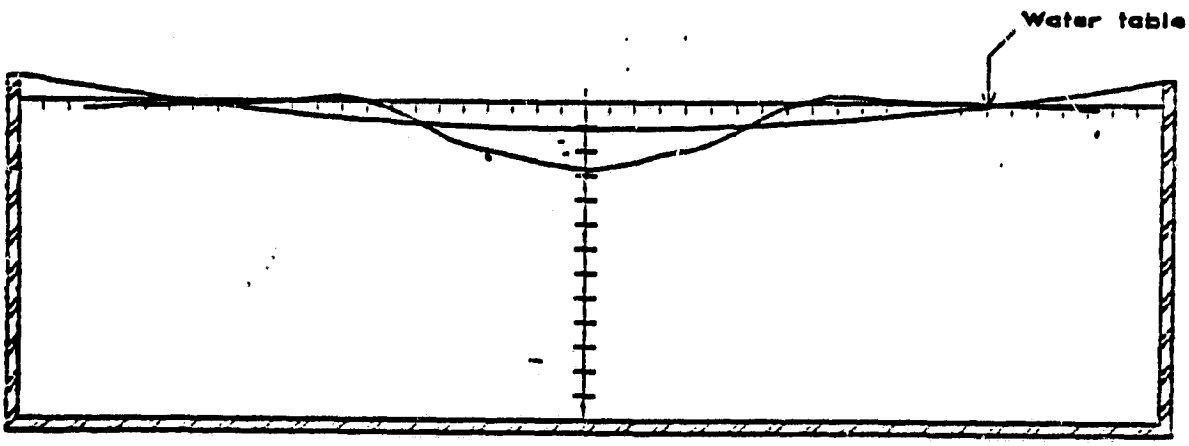

Lets Look at the raw data for

WATER CAVITY GROWTH VS GRAVITY

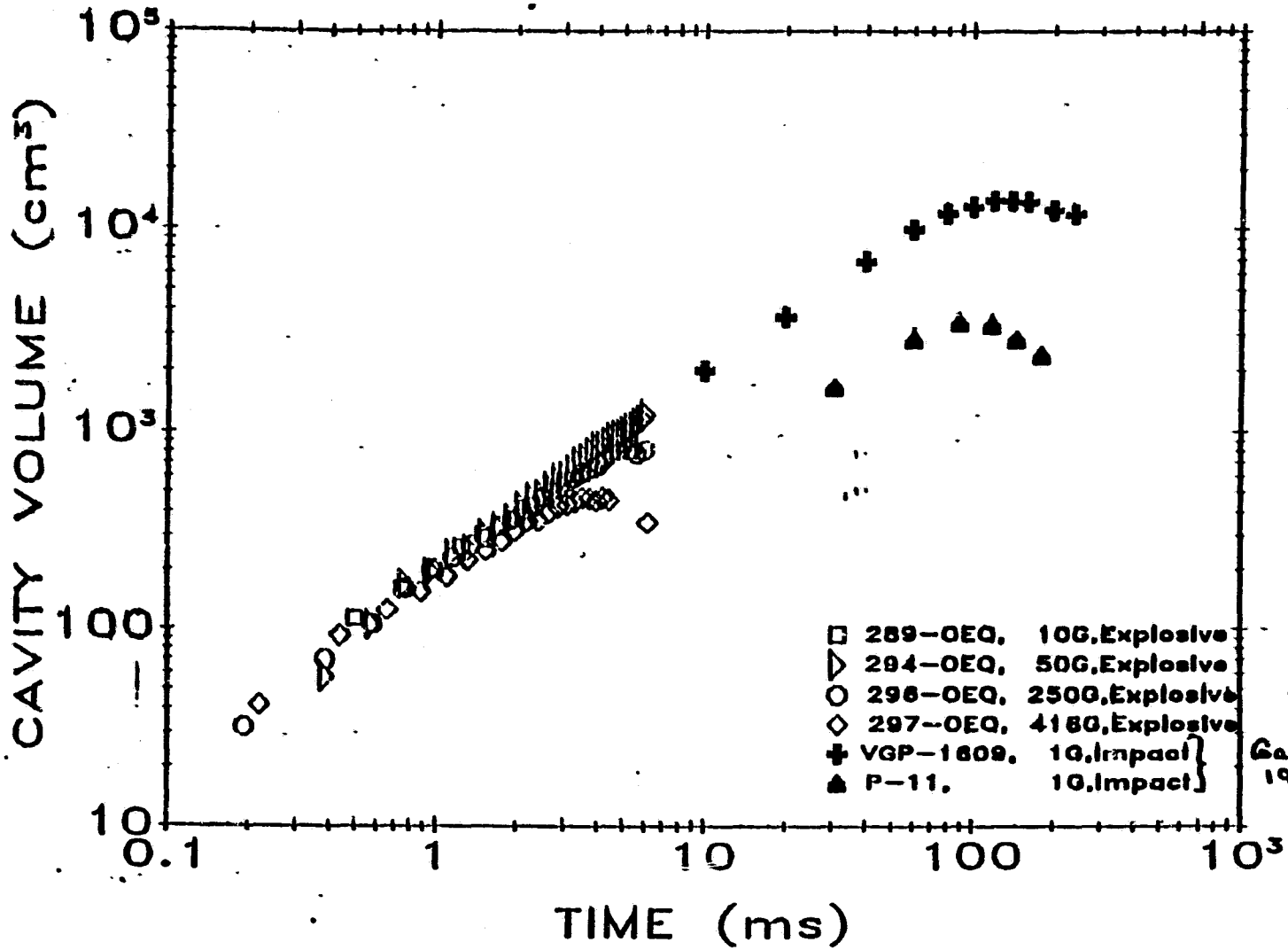

Gault & Sonett 1982

ORIGINAL PAGE IS OF POOR QUALITY

Maximum Crater Volume V_G

GAULT WATER DATA

REG #	CONST	(C.F.)	α SLOPE	(S.D.)	RSQUARE	F
1	2.1008	(1.851)	-.65096	(.03308)	.97974	7.8378

$$\pi_V = A\,\pi_2^{-\alpha}$$

$$V\rho / 4.19\,a^3\delta = A\,(3.22\,ga/v^2)^{-\alpha}$$

$$V_G = 4.11\,(\delta/\rho)\,(a\,v^{\frac{2\alpha}{3-\alpha}})^{3-\alpha}\,g^{-\alpha}$$

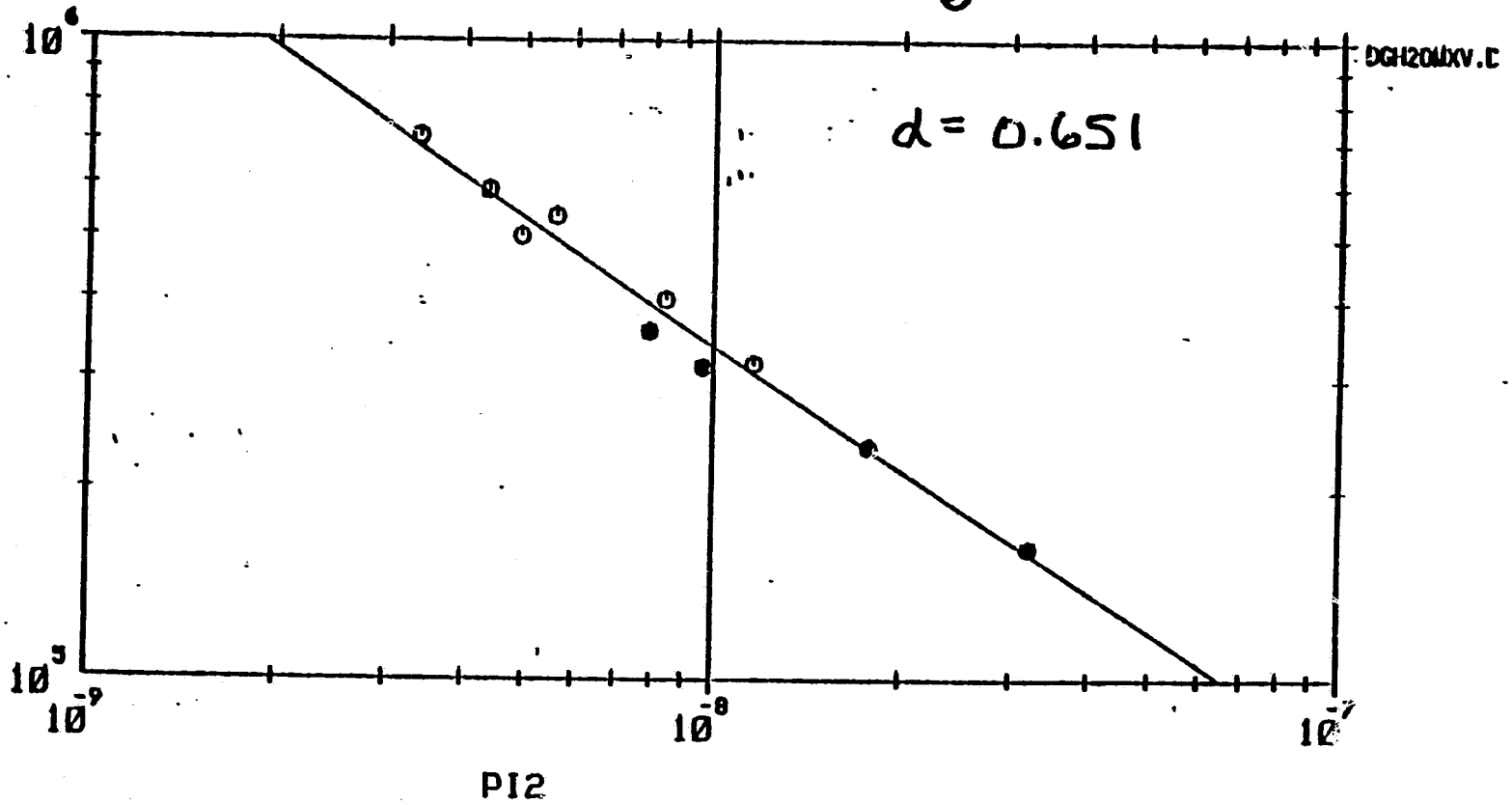

ORIGINAL PAGE IS OF POOR QUALITY

Time of Formation T_G

GAULT WATER DATA

REQ #	CONST	(C.F.)	τ SLOPE	(S.D.)	RSQUARE	F
1	1.7981	(1.2938)	-.60264	(.01384)	.99579	7.9689

$$\pi_T = B\,\pi_2^{-\tau} \qquad T U/a = \sqrt{2}\,B\,(3.22\,ga/U^2)^{-\tau}$$

$$T_G = 1.26\left(a\,U^{\frac{2\tau-1}{1-\tau}}\right)^{1-\tau} g^{-\tau}$$

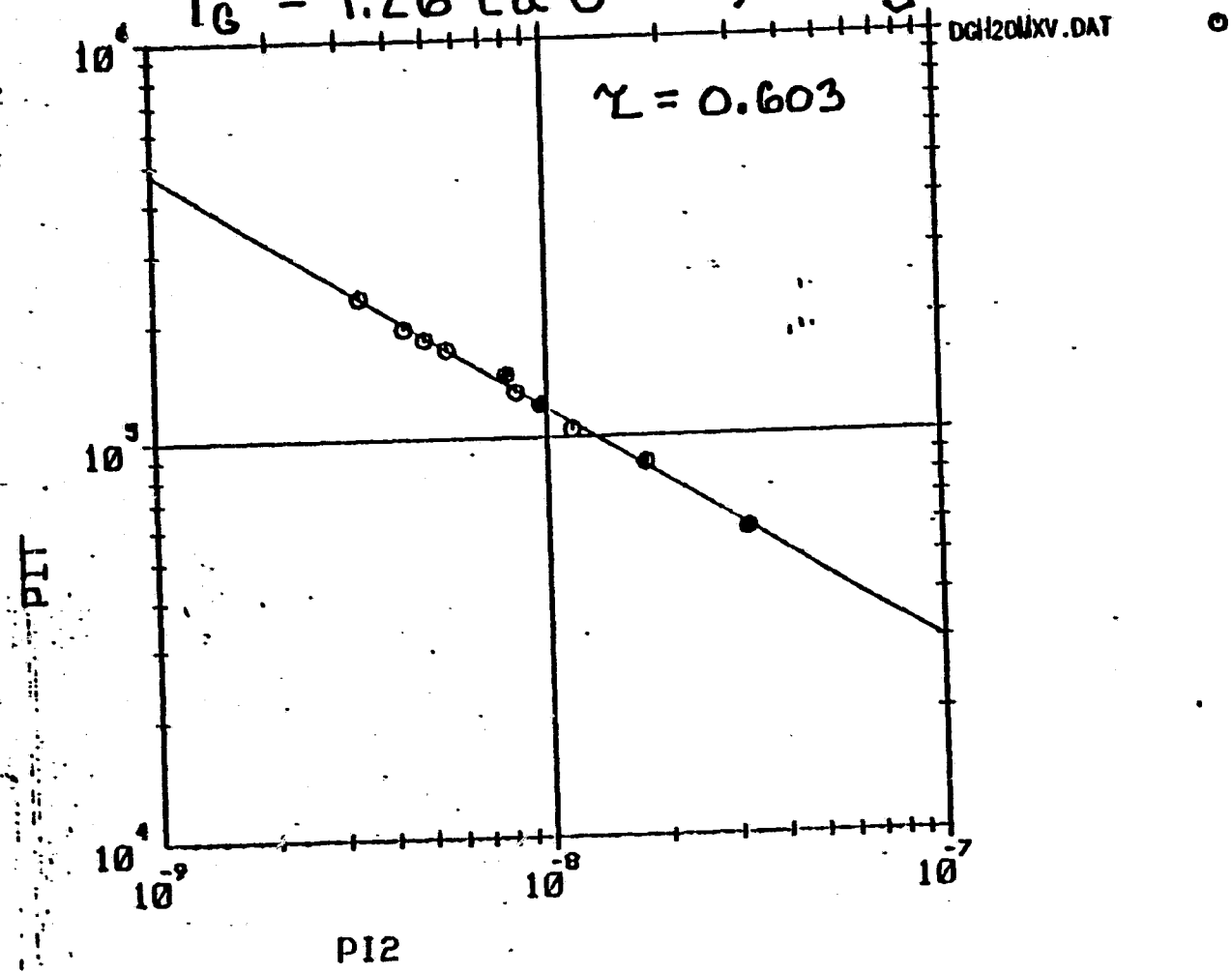

ORIGINAL PAGE IS
OF POOR QUALITY

If a unique coupling parameter determines both V_G and T_G

GAULT WATER DATA

REG #	CONST	(C.F.)	SLOPE	(S.D.)	RSQUARE	F
1	1.2431	(2.2744)	1.071	(.06963)	.96728	7.7380

$$a V^{\frac{2\alpha}{3-\alpha}} = a V^{\frac{2\tau-1}{1-\tau}} \Rightarrow \tau = \frac{3+\alpha}{6}$$

$$\pi_V = C\,\pi_T^{\alpha/\tau} = C\,\pi_T^{\frac{6\alpha}{3+\alpha}}$$

$$\alpha = 0.651 \qquad \frac{6\alpha}{3+\alpha} = 1.070$$

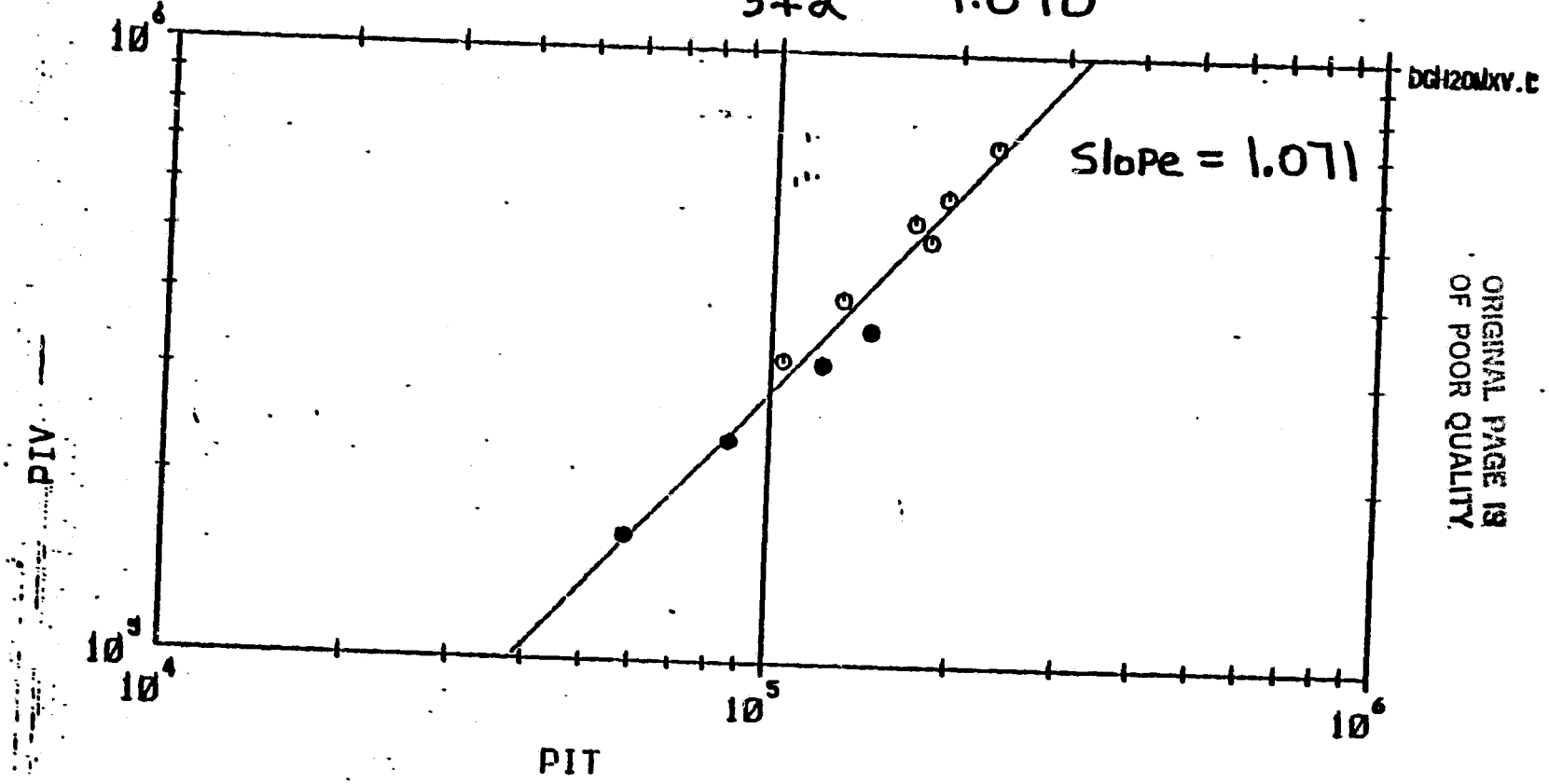

ORIGINAL PAGE IS OF POOR QUALITY

Dimensional Analysis

6

<u>max volume</u> $V_G = f(a, U, \delta, \rho, g)$

coupling parameter $C = f(a, U, \delta)$

hence $V_G = f(C, \rho, g) \Rightarrow$ Power law

<u>crater growth</u> $V(t) = f(C, \rho, g, t)$

invert V_G $C = f(V_G, \rho, g)$

hence $V(t) = f(V_G, \cancel{\rho}, g, t)$ density out

forming π-groups

$$\frac{V(t)}{V_G} = \mathcal{F}\left(\frac{t\sqrt{g}}{V_G^{1/6}}\right)$$

ORIGINAL PAGE IS
OF POOR QUALITY

Dimensional Analysis (cont.)

Likewise for Time of Formation

$$T_G = f(a, V, \delta, \rho, g)$$

$$T_G = f(C, \rho, g)$$

Replace C with V_G

$$T_G = f(V_G, \cancel{\rho}, g)$$

Can write a single π-group

$$\frac{T_G\sqrt{g}}{V_G^{1/6}} = \text{constant} \qquad T_G \propto \left(\frac{V_G}{g^3}\right)^{1/6}$$

ORIGINAL PAGE IS
OF POOR QUALITY

Experimental Data Supports: $T_G \propto \left(\frac{V_G}{g^3}\right)^{1/6}$

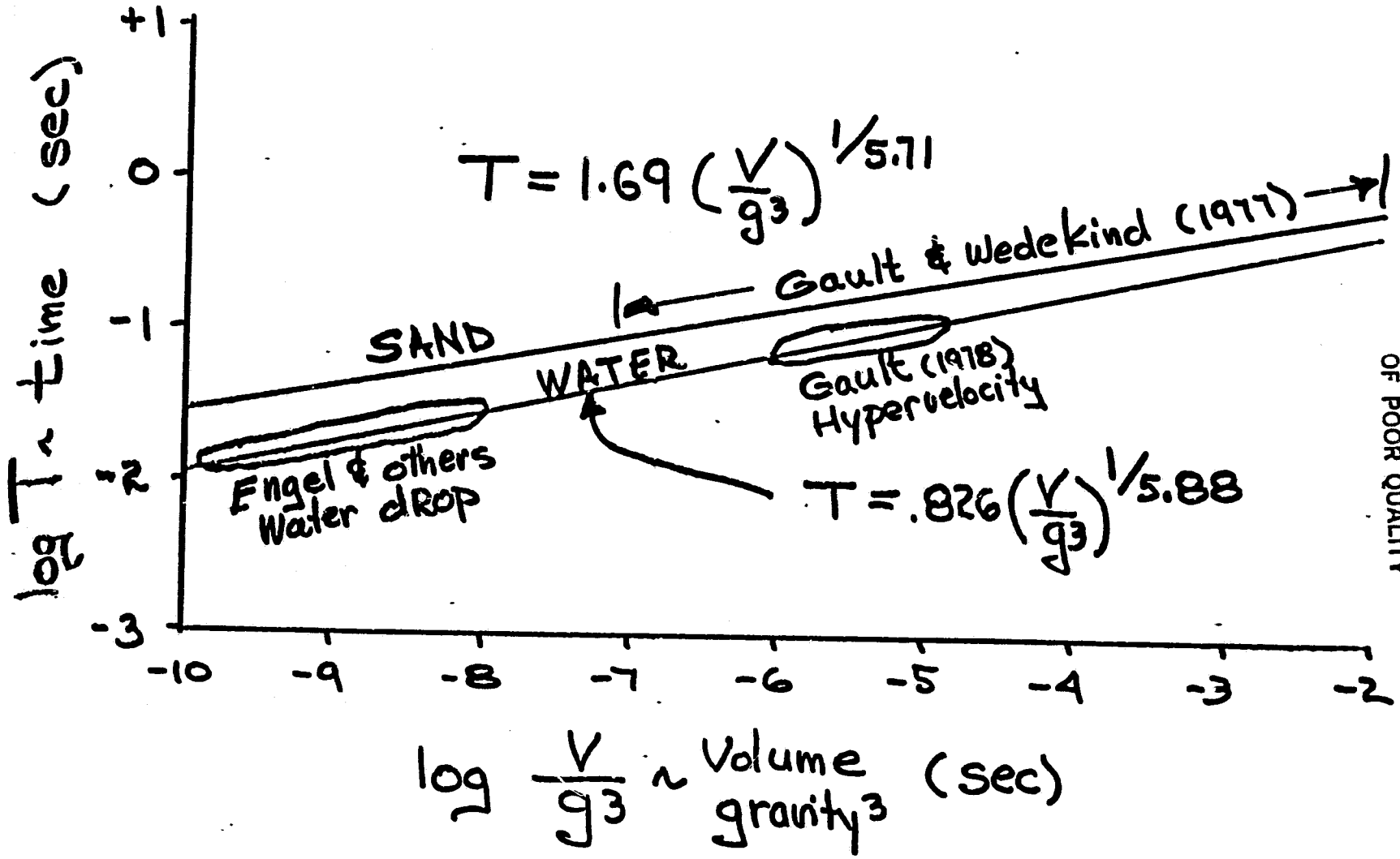

1σ bounds
1/5.60 – 1/5.81
1/5.77 – 1/6.02

ORIGINAL PAGE IS OF POOR QUALITY

Kinematic Equivalence

now replace $V_G^{1/6}$ with $T_G\sqrt{g}$

to get final result

$$\boxed{\frac{V(t)}{V_G} = f\left(\frac{t}{T_G}\right)}$$

ORIGINAL PAGE IS
OF POOR QUALITY

max volume $V_G = A'(\delta/\rho)\left(aU^{\frac{2\alpha}{3-\alpha}}\right)^{3-\alpha} g^{-\alpha}$

form. time $T_G = B'\left(aU^{\frac{2\chi-1}{1-\chi}}\right)^{1-\chi} g^{-\chi}$

10

GRAVITY-SCALED WATER CAVITY GROWTH

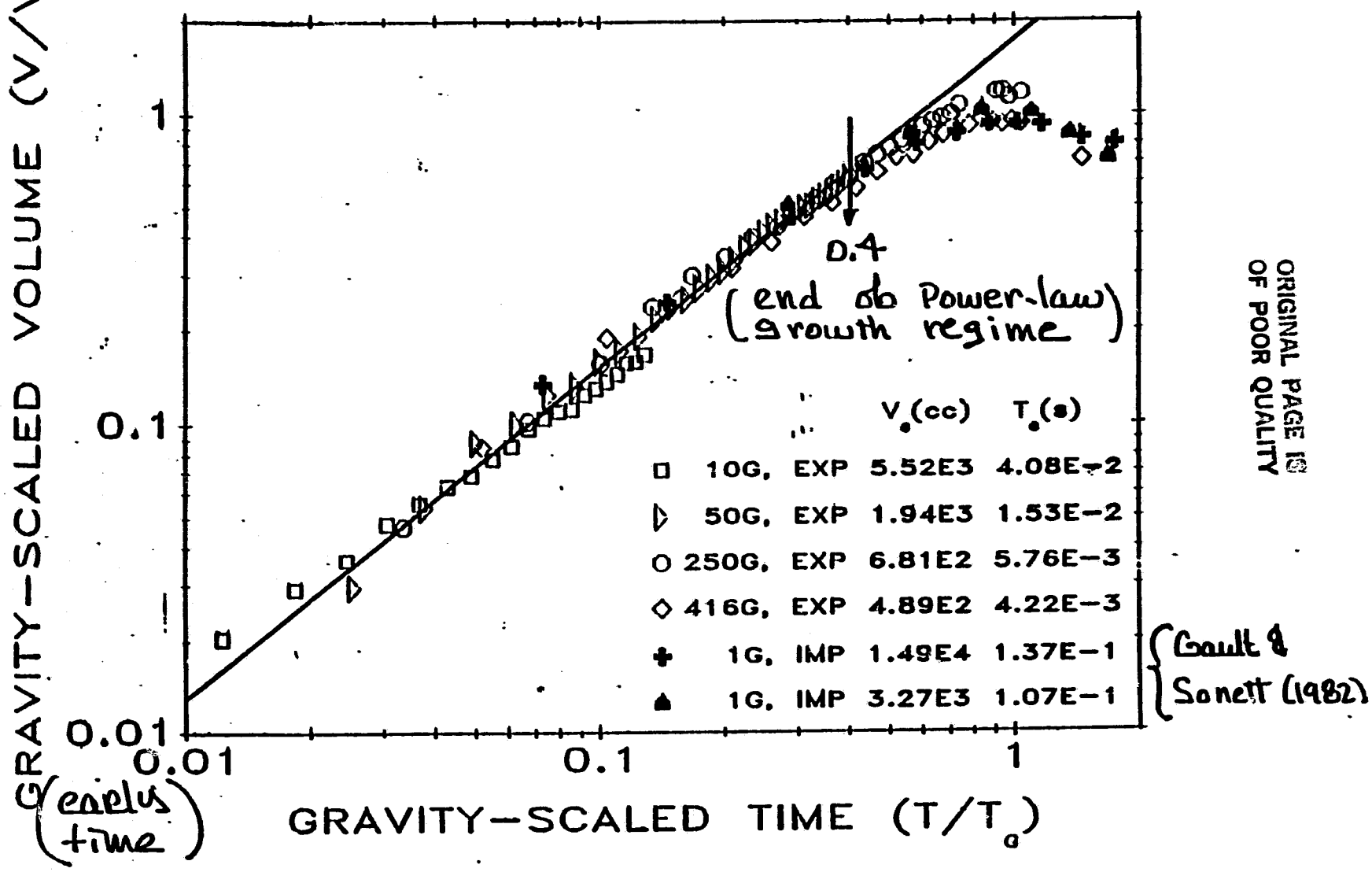

ORIGINAL PAGE IS OF POOR QUALITY

Conclusions for near-surface explosions and impact into water

① Rate of growth is determined by single global function:

$$V^* = \mathcal{F}(T^*)$$

$$V^* = V(t)/V_G = V(t)/V_{final}$$

$$T^* = t/T_G = t/T_{final}$$

② In principle, any one event can be used to define $\mathcal{F}$.

③ All water craters are kinematically similiar.

ORIGINAL PAGE IS OF POOR QUALITY

Water Crater Conclusions (cont.)

4. Gravity arrest of crater growth begins at $T^* \approx 0.4$

5. Prior to that gravity has no influence and growth rate is Power-law.

6. "Very-early time" effects are limited to $T^* = V^* < 0.01$

7. Next step is to examine other targets, wet and dry soils to look for same features.

ORIGINAL PAGE IS
OF POOR QUALITY

P42-11

[illegible] SCALING OF IMPACT CRATER GROWTH

K.A. Holsapple and M.W. Bjorkman
(The Boeing Company, M/S 13-20, Seattle, WA 98124)
(Sponsor: H.H. Schmidt)

Calculations and experiments of crater time histories are compared to predictions of the coupling parameter theory. In the intermediate time regime data should be scaled with length $d_c = a(U/c)^{\nu}(\delta/\rho)^{\nu}$, and with time $t_c = (a/U)(U/c)^{1+\nu}(\delta/\rho)^{\nu}$. The figure shows two sets of calculations of impacts into metals, calculations of impacts into gabbroic anorthosite, and experimental data for impacts into water and into aluminum, with wide ranges of the independent variables. All data superimpose along a common curve except for the very early stages before the coupling parameter characterizes the problem, and for the very late stages where either material strength (metals and rocks) or gravity (water) acts to limit the crater.

For the late-stages of strength-dominated materials, the appropriate scaling is a length scale $d_y = a(\delta U^2/\gamma)^{\nu/2}(\delta/\rho)^{\nu-\nu/2}$ and a time scale $t_y = (a/U)(\delta U^2/\gamma)^{(\nu+1)/2}(\delta/\rho)^{(2\nu-\nu-1)/2}$. In this form the data superimpose in the late stages, as will be presented. Gravity-scaled results are presented in another paper of these proceedings.

ORIGINAL PAGE IS
OF POOR QUALITY

IMPACT CRATERING MECHANICS

Understanding and Comparing Problems

I. VARIABLES

ANY Dependent Variable: Volume, Time of Formation, Melt Volume, Dynamic Growth, etc.

Depends Upon

Impactor
- Radius, a
- Velocity, U
- High Pressure properties, P_I: δ, K_I,...

Target
- High Pressure properties, P_T: ρ, K_T, ε_m,...
- Low Pressure properties, Y,...

Environment
- Gravity, g
- Atmosphere properties, P_A

ORIGINAL PAGE IS OF POOR QUALITY

II. REGIMES OF INFLUENCE
(Separation of Variables)

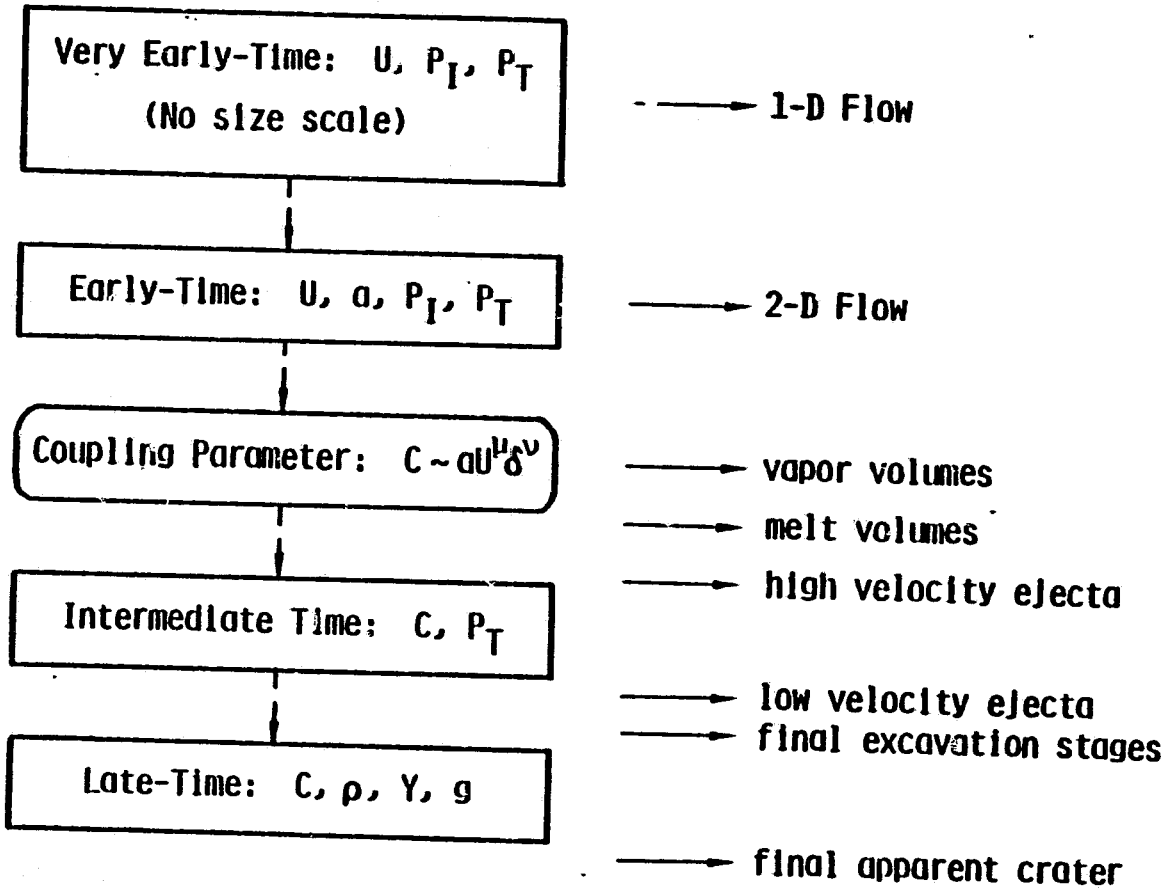

REGIMES OF CRATER GROWTH

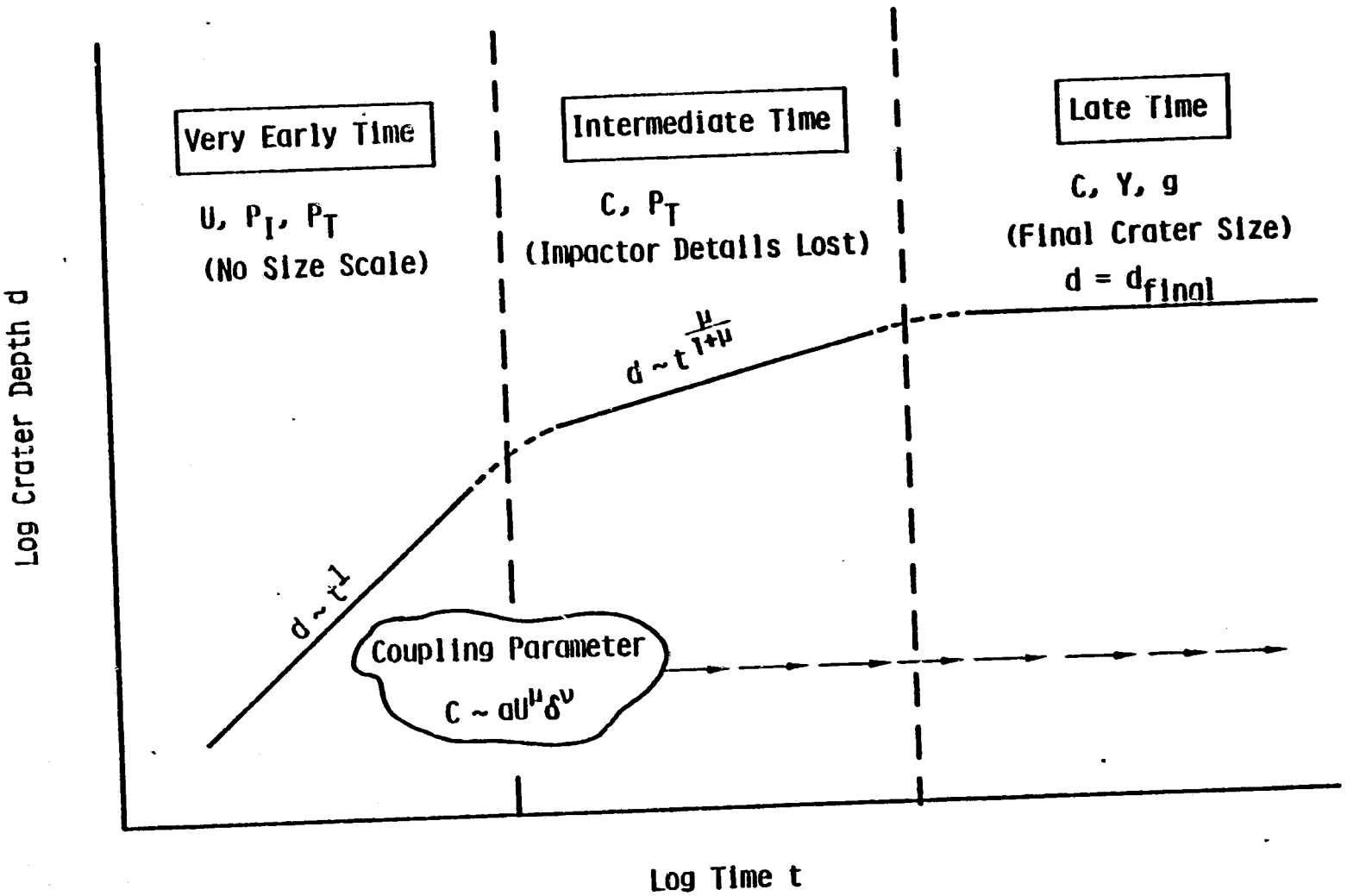

ORIGINAL PAGE IS
OF POOR QUALITY

crater growth curves: unscaled

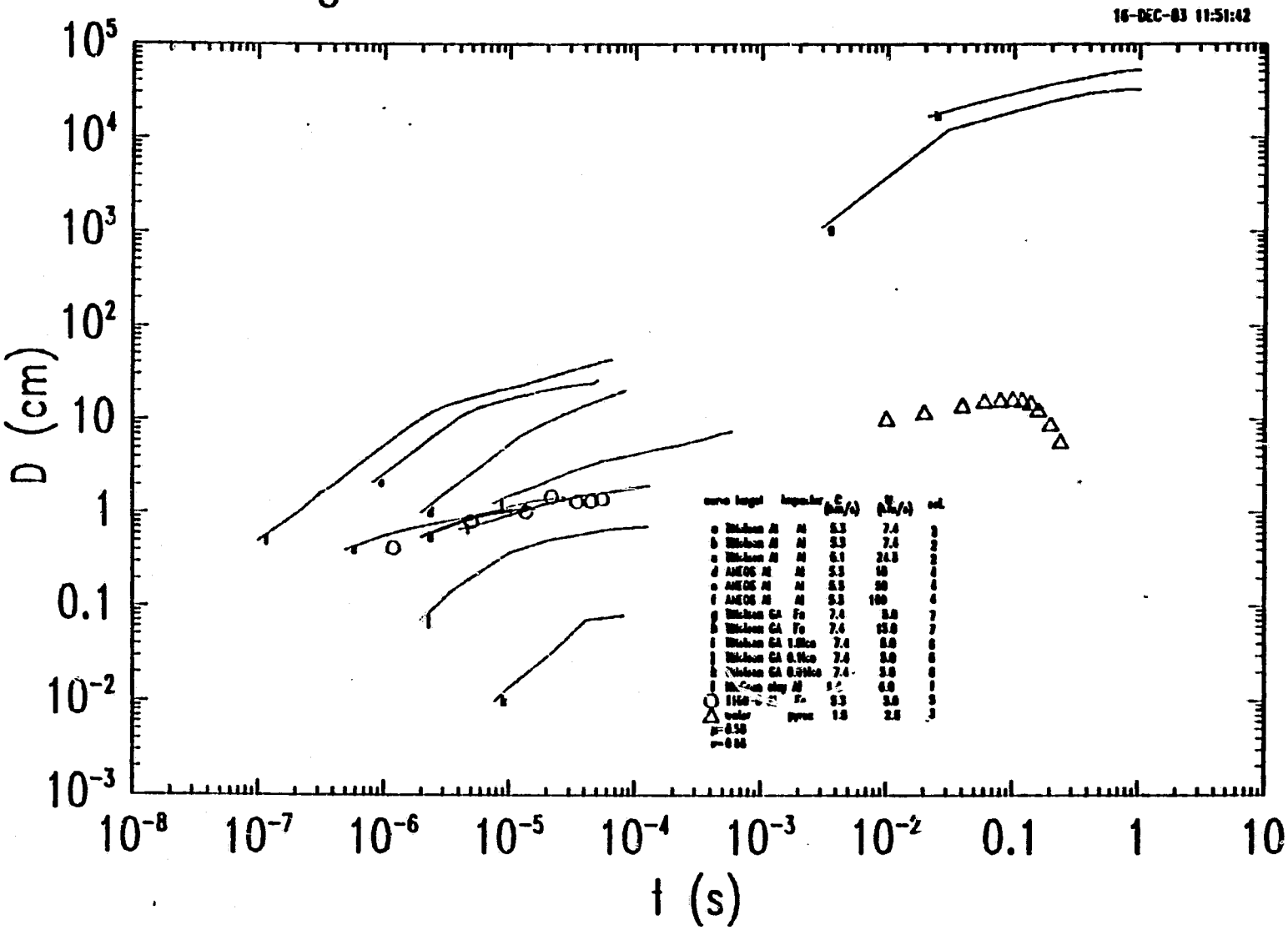

ORIGINAL PAGE IS
OF POOR QUALITY

III. RESULTS

- Early-Time $d = F(t, U, P_I, P_T)$

  Initial 1-D particle velocity $v = v(U, P_I, P_T)$

  $\therefore\ d = F(t, v)$

  $\therefore\ \boxed{d \propto vt}$ all materials

crater growth curves: early time

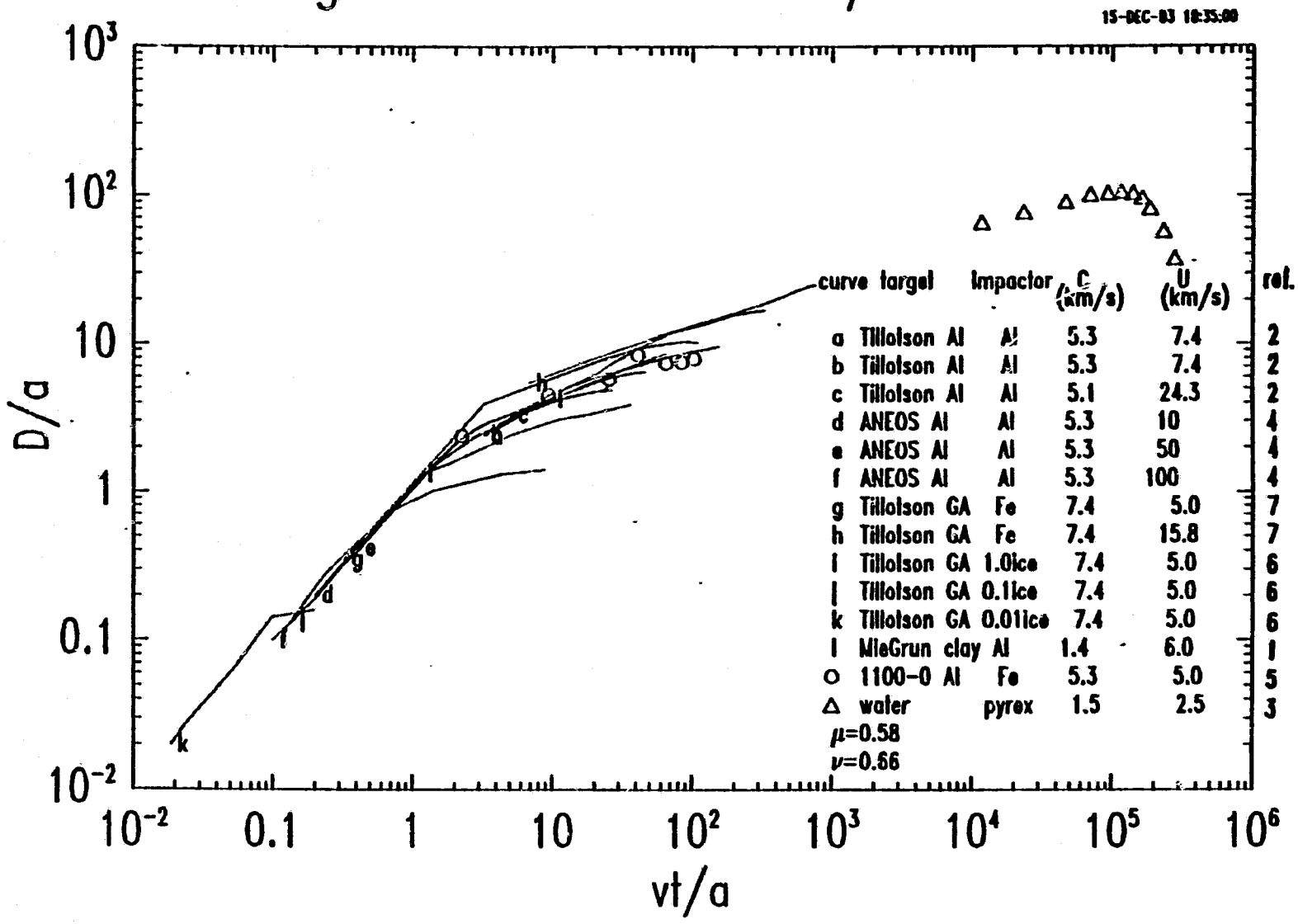

ORIGINAL PAGE IS
OF POOR QUALITY

III. RESULTS (Continued)

- Intermediate-Time $d = F(t, C, P_T)$

Try P_T: ρ, c .

$\therefore \; d = F(t, C, \rho, c)$

$$\therefore \; \frac{d}{d_c} = F\left(\frac{t}{t_c}\right) \qquad d_c = a\left(\frac{U}{c}\right)^{\mu}\left(\frac{\delta}{\rho}\right)^{\nu}$$

$$t_c = \left(\frac{a}{U}\right)\left(\frac{U}{c}\right)^{1+\mu}\left(\frac{\delta}{\rho}\right)^{\nu}$$

Try P_T: ρ

$\therefore \; d = F(t, C, \rho)$

$$\therefore \; \boxed{\frac{d}{d_c} \propto \left(\frac{t}{t_c}\right)^{\frac{\mu}{1+\mu}}} \qquad \text{Power-Law}$$

ORIGINAL PAGE IS
OF POOR QUALITY

:intermediate-time scaling

6-DEC-93 13:50:56

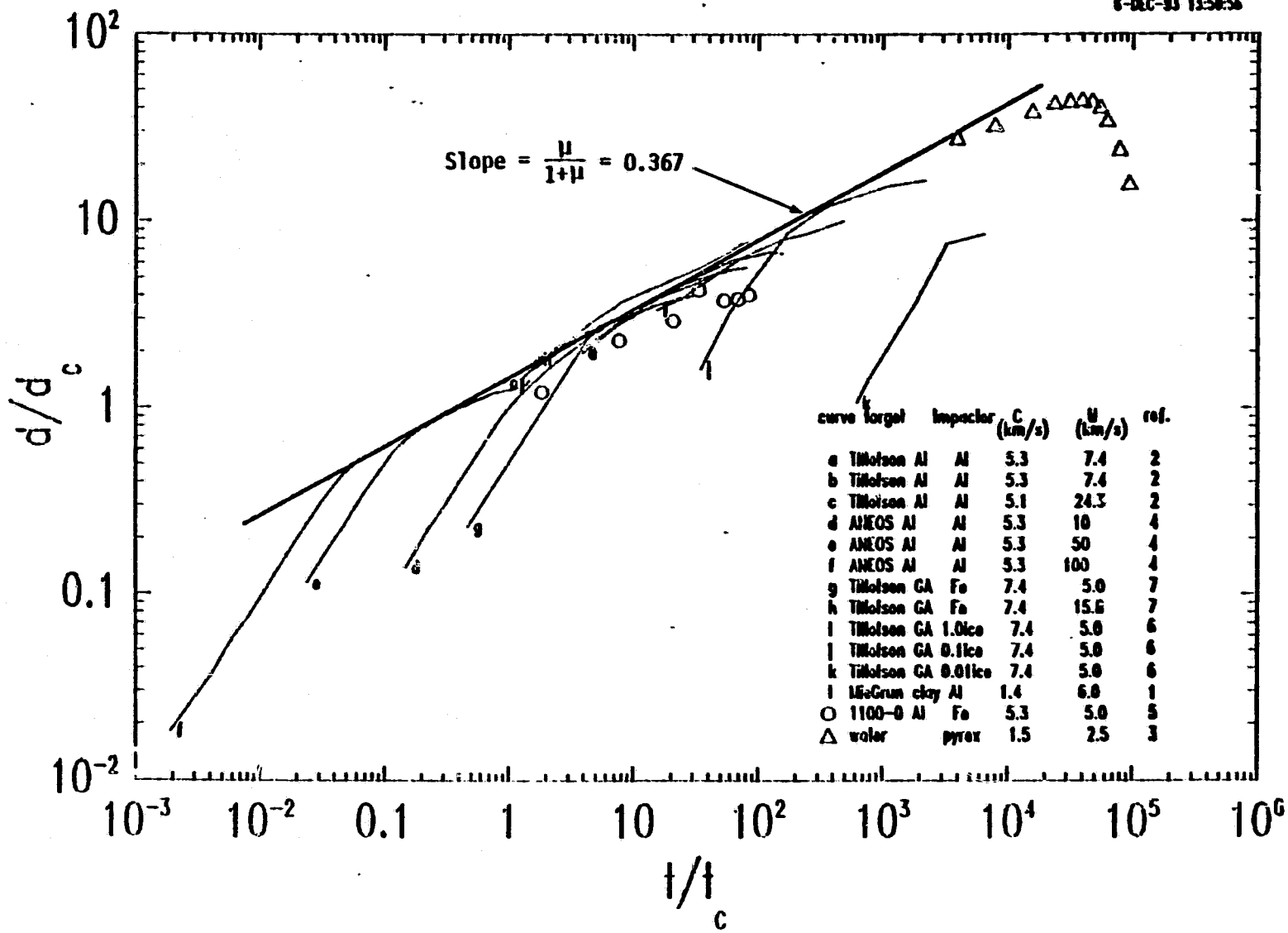

ORIGINAL PAGE IS
OF POOR QUALITY

crater growth curves: early--time scaling

6-DEC-83 13:30:38

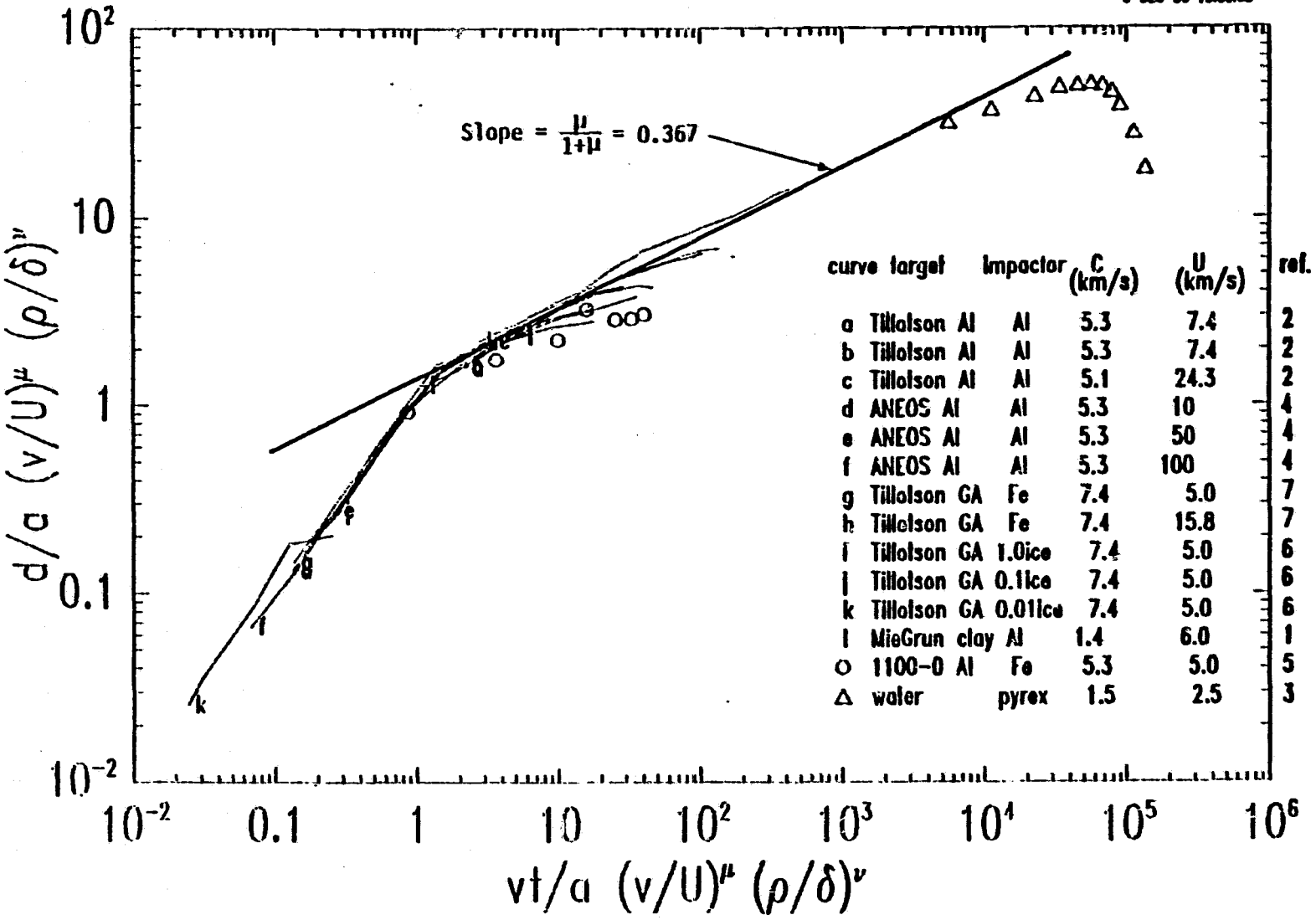

curve	target	impactor	C (km/s)	U (km/s)	ref.
a	Tillotson Al	Al	5.3	7.4	2
b	Tillotson Al	Al	5.3	7.4	2
c	Tillotson Al	Al	5.1	24.3	2
d	ANEOS Al	Al	5.3	10	4
e	ANEOS Al	Al	5.3	50	4
f	ANEOS Al	Al	5.3	100	4
g	Tillotson GA	Fe	7.4	5.0	7
h	Tillotson GA	Fe	7.4	15.8	7
i	Tillotson GA	1.0ice	7.4	5.0	6
j	Tillotson GA	0.1ice	7.4	5.0	6
k	Tillotson GA	0.01ice	7.4	5.0	6
l	MieGrun clay	Al	1.4	6.0	1
o	1100-0 Al	Fe	5.3	5.0	5
Δ	water	pyrex	1.5	2.5	3

ORIGINAL PAGE IS
OF POOR QUALITY

III. RESULTS (Continued)

- Late-Time: Final Crater Size

$$d_{final} = F(C, \rho, Y, g)$$

$$t_{final} = F(C, \rho, Y, g)$$

Strength Regime: (g out)

$$d_Y = F(C, \rho, Y) \qquad t_Y = F(C, \rho, Y)$$

$$d_Y \propto a \left(\frac{\rho U^2}{Y}\right)^{\mu/2} \left(\frac{\delta}{\rho}\right)^{\nu}$$

$$t_Y \propto \left(\frac{a}{U}\right)\left(\frac{\rho U^2}{Y}\right)^{\frac{\mu+1}{2}} \left(\frac{\delta}{\rho}\right)^{\nu}$$

Power Laws

Gravity Regime: (Y out)

$$d_g \propto a \left(\frac{U^2}{ga}\right)^{\frac{3\mu}{2+\mu}} \left(\frac{\delta}{\rho}\right)^{-}$$

$$t_g \propto \left(\frac{a}{U}\right)\left(\frac{U^2}{ga}\right)^{\frac{1+\mu}{2+\mu}} \left(\frac{\delta}{\rho}\right)^{-}$$

Previous $\alpha = \frac{3\mu}{2+\mu}$, $\mu = \frac{2\alpha}{3-\alpha}$

ORIGINAL PAGE IS
OF POOR QUALITY

crater growth curves: late-time scaling

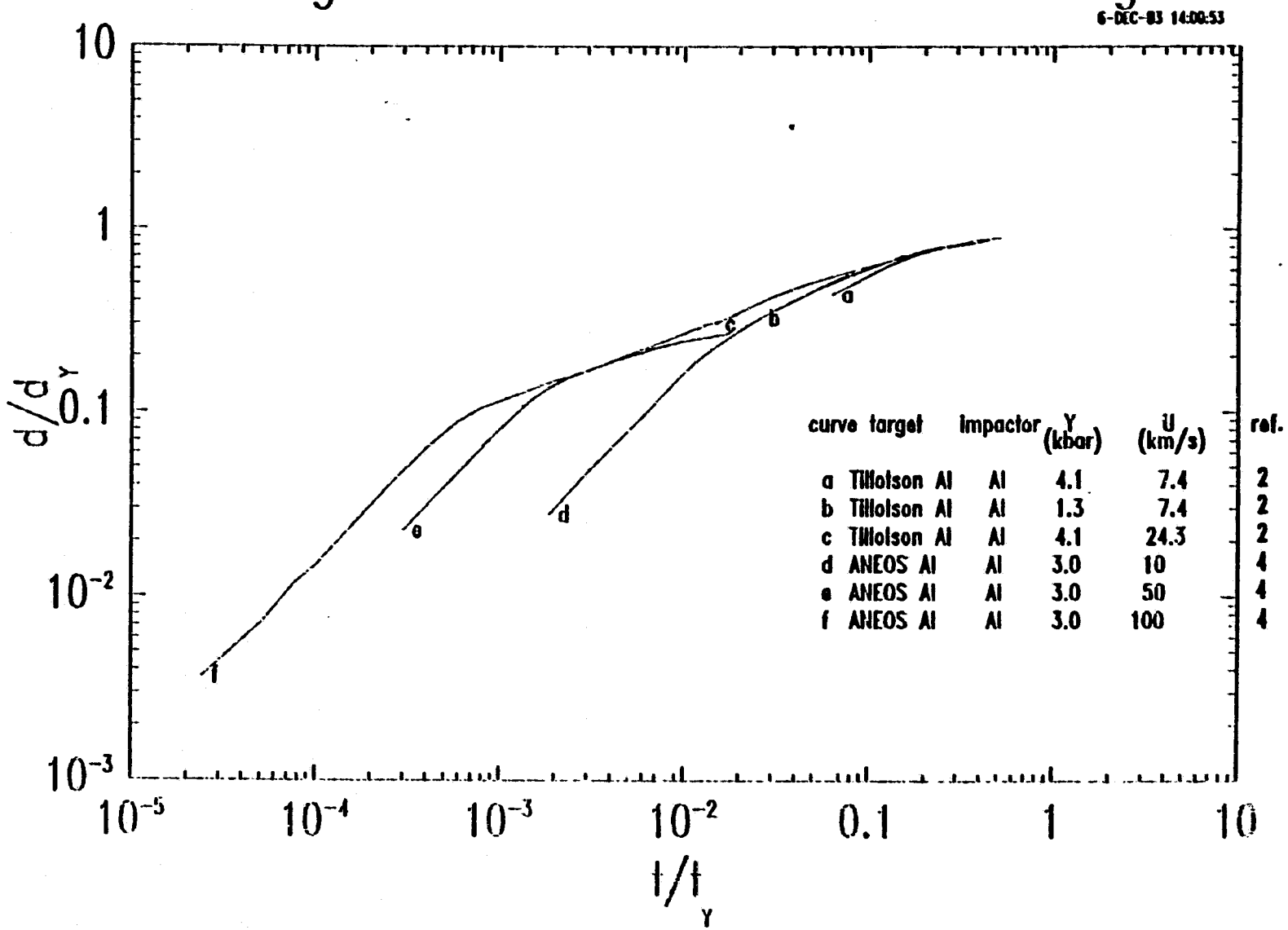

ORIGINAL PAGE IS
OF POOR QUALITY

IV. SUMMARY

- There are simple scaling laws that superimpose quite diverse impact problems:

  - Projectiles: Ice, Al, Fe, Pyrex
  - Targets: Al, GA, Clay, Water

  } All Non-Porous

  - Velocities: 2.5 to 100 Km/sec

- A very simple measure $C \sim aU^{\mu}\delta^{\nu}$ of the projectile governs the process after all except very early times.

- This coupling parameter uniquely determines all intermediate and late-time scaling laws.

REFERENCES

1. M. G. Austin, J. M. Thomsen, S. F. Ruhl, D. L. Orphal, and P. H. Schultz. Calculational Investigation of Impact Cratering Dynamics: Material Motions During the Crater Growth Period, in Proceedings of the 11th Lunar and Planetary Science Conference (1980), pp. 2325-45.

2. J. K. Dienes and J. M. Walsh. Theory of Impact: Some General Principles and the Method of Eulerian Codes, in High Velocity Impact Phenomena, ed. by R. Kinslow, Academic Press, New York, 1970, pp. 45-104.

3. D. E. Gault and C. P. Sonett. Laboratory Simulation of Pelagic Asteroidal Impact: Atmospheric Injection, Benthic Topography and the Surface Wave Radiation Field, in Conference on Large Body Impacts and Terrestrial Evolution: Geological, Climatological, and Biological Implications (1981: Snowbird, Utah) Geological Implications of Large Asteroids and Comets on the Earth.

4. K. A. Holsapple, unpublished.

5. J. H. Kineke. Observations of Crater Formation in Ductile Materials, in Proceedings of the 5th Symposium on Hypervelocity Impact, vol. 1, part 2, October - November, 1961, pp. 339-70.

6. J. D. O'Keefe and T. J. Ahrens. Cometary and Meteorite Swarm Impact on Planetary Surfaces, Journal of Geophysical Research (1982).

7. D. L. Orphal, W. F. Borden, S. A. Larson, and P. H. Schultz. Impact Melt Generation and Transport, in Proceedings of the 11th Lunar and Planetary Science Conference (1980), pp. 2309-23.